Organic−Inorganic Hybrid from Ionomer via Sol−Gel Reaction

Yan Gao,[†] Namita Roy Choudhury,*[,†] Naba Dutta,[†] Jani Matisons,[†] Mike Reading,[‡] and Luc Delmotte[§]

Polymer Science Group, Ian Wark Research Institute, University of South Australia, Mawson Lakes, South Australia 5095, Australia, Institute of Polymer Technology and Materials Engineering, Loughborough University, Loughborough LE11, 3TU, U.K., and Ecole National Superior de Chimie de Mulhouse, Mulhouse, F-68093 France

Received March 8, 2001. Revised Manuscript Received June 26, 2001

Transparent organic−inorganic hybrid material was synthesized via the sol−gel method using polyethylene-***co***-Zn-acrylic acid (Zn−PEAA) ionomer and a metal alkoxide, tetraethyl orthosilicate (TEOS). The resulting material was characterized using various spectroscopic, microscopic, and thermal techniques. Photoacoustic Fourier transform infrared spectroscopy (PA-FTIR) and ^{29}Si solid-state nuclear magnetic resonance spectroscopy (^{29}Si solid-state NMR) results prove that silica is formed via the sol−gel reaction. Scanning electron microscopy with energy-dispersive X-ray analysis (SEM-EDAX), transmission electron microscopy (TEM), and atomic force microscopy (AFM) studies indicate that silica particle size is in nanoscopic level (50 nm average size), and silica nanoparticles are uniformly dispersed in the polymer matrix after the sol−gel process. Thermogravimetric analysis (TGA) results show that the silica content of the hybrid is about 19%. The thermal stability of the ionomer increases after hybridization. The crystallinity of the hybrid material is found to decrease from modulated differential scanning calorimetry (MDSC) and wide-angle X-ray scattering (WAXS) results. Dynamic mechanical analysis (DMA) of the hybrid shows that the storage modulus of ionomer increases after the sol−gel reaction, and the order−disorder transition temperature of the ionic cluster also increases, indicating the existence of silica mostly in the microphase separated cluster template.

Introduction

Hybridization is an important and evolutionary route for the growth of a strong polymer−filler interface. The concept consists of deriving a hybrid from two generically different constituent materials, such as organic and inorganic, at a molecular level dispersion. The most popular, practical approach for preparing organic−inorganic hybrids is by sol−gel reaction.[1−5] The sol−gel process with its unique mild processing characteristics can be used to prepare pure and well-controlled compositions. The process involves the hydrolysis of metal alkoxides, followed by a condensation reaction to produce metal oxides. Silicon alkoxide, e.g., tetraethyl orthosilicate (TEOS) and tetramethyl orthosilicate (TMOS), and the silica therefrom are the most widely used metal alkoxides by far.

Depending on the strength or level of interaction[1,6] between these organic−inorganic phases, there are two types of hybrid materials: class I hybrid involving physical or weak phase interaction, e.g., hydrogen bonding, van der Waals or simple mechanical mixing, and class II hybrid possessing a strong chemical or covalent or iono-covalent bond between the organic and inorganic phases.[1,6−8] However, the method most commonly used for hybrid preparation is via hydrogen bonding between the polar functional group of the polymer and the residual silanol group of silica.[9] The utilization of ionic interaction to synthesize nanoscale hybrid recently was reported by Chujo et al.[10] Intercalation of an organic compound into a metal oxide layer was also achieved by Krishnamoorti et al.[11] using ionic interaction. Since the strength of ionic interaction is much higher than that of hydrogen bonding, therefore it should allow a better degree of homogeneity and order in the final hybrid.

The goal of both sol−gel and intercalation ultrastructure processes is to control the surface and interface of

* To whom correspondence should be addressed. Phone: 61 8 8302 3719. Fax: 61 8 8302 3755. E-mail: Namita.Choudhury@unisa.edu.au.
† University of South Autralia.
‡ Loughborough University.
§ Ecole National Superior de Chimie de Mulhouse.

(1) Wen, J.; Wilkes, G. L. *Chem. Mater.* **1996**, *8*, 1667.
(2) Novak, B.; Ellsworth, M. W.; Verrier, C. In *Hybrid Organic−Inorganic Composites*; Mark, J. E., Lee, C.Y−C., Bianconi, P. A., Eds.; ACS Symposium Series 585; American Chemical Society: Washington, DC, 1995; p 86.
(3) Mark, J. E.; Jiang, C. Y.; Wilkes, G. L. *Macromolecules* **1984**, *17*, 2613.
(4) Schubert, U.; Husing, N.; Lorens, A. *Chem. Mater.* **1995**, *7*, 2010.
(5) Wilkes, G. L.; Wen, J. In *Polymeric Materials Encyclopedia*; Salamone, J. C., Ed., CRC Press: New York, 1996; Vol. 6, p 4782.
(6) Nell, J. L.; Wilkes, G. L.; Mohanty, D. K. *J. Appl. Polym. Sci.* **1990**, *40*, 1177.
(7) Ellsworth, M. W.; Novak, B. M. *J. Am. Chem. Soc.* **1991**, *113*, 2756.
(8) Novak, B. M. *Macromolecules* **1991**, *24*, 5481.
(9) Chujo, Y.; Ihare, E.; Kore, S.; Saegusa, T. *Macromolecules* **1993**, *26*, 5681.
(10) Tamaki, R.; Chujo, Y. *Chem. Mater.* **1999**, *11*, 1719.
(11) Krishnamoorti, R.; Vaia, R. A.; Giannelis, E. P. *Chem. Mater.* **1996**, *8*, 1728.

10.1021/cm010179s CCC: $20.00
Published on Web 09/13/2001

the materials during the earliest stage of synthesis. Much work was also performed in the past few years to form ordered hybrids via self-assembly.[12−16] Molecular self-assembly uses the interactive forces of solid-state lattice structures, chemical bonds, and van der Waals interactive forces to form large aggregates of atomic or molecular units with specific geometry. By far, most of the work has been done with conjugated polymers for electroluminescent applications, since the constrained environment provided by the layered host is expected to lead to a high degree of polymer ordering and hence useful optical properties.

Among other polymers, ionomers[17] are remarkable materials because of their unusual cluster morphology. Such morphology could be an attractive template for the synthesis and ordering of the ceramic phase. Generally, the ionic groups are aggregated in well-ordered domains (clusters) with the remainder dispersed in the matrix (multiplets) of low dielectric constant, but do not themselves constitute a second phase. The number of ion pairs in a multiplet is sterically limited by the salt amount bound to the polymer chain, and the clusters are small microphase separated regions of aggregated multiplets. Thus, the clusters are rich in ion pairs, together with some organic polymer. They can confine a small reactant molecule in the vicinity of the metal cation. These clusters or well-ordered domains can thus be used as a nanoreactor for the synthesis of colloidal inorganic particles in the polymer. Mauritz et al.[18] followed the microstructure evolution of the highly dispersed silicon oxide phase, using the in-situ sulfonic acid catalyzed sol−gel reaction of Nafion (PFSI-perfurosulfonic acid ionomer) membrane, and observed the persistence of the polar−nonpolar nanophase separated template of the ionomer despite the evolution of a silicon oxide phase.

The properties of such hybrid networks strongly depend on various parameters such as the degree of phase dispersion, the relative amount of organic and inorganic components, the type of catalyst, the molar ratio of water to silane, the reaction time, temperature, and ionic strength of the sol as well as the molecular weight of the polymer. Many hybrids have been reported in the literature based on poly(methyl methacrylate),[19] polyimide,[13] poly(dimethysiloxane),[14] etc. However, very few organic−inorganic hybrid materials are reported so far that are based on ionomer.[20] Tamaki and Chujo[10] synthesized nanoscale homogeneous polystyrene and silica gel polymer hybrids using a sulfonated polystyrene ionomer as the organic polymer and (3-aminopropyl)-trimethoxysilane (APTMOS) as the countercation precursor for the inorganic phase. Recently, Zeng et al.[21] prepared ionomers with lead (Pb^{2+}) ions and subsequently lead oxide (PbO) nanoparticles within the matrix using a solid−gas reaction.

Despite all their inherent advantages, the reports on ionomer−inorganic hybrid materials remain scanty, due to their very poor solubility in solvents. In this work, we report a new Zn−PEAA−silica (Zn−PEAA − polyethylene-*co*-Zn-acrylic acid) hybrid material prepared by the sol−gel process. The hybrid material was characterized by scanning electron microscopy coupled with energy dispersive X-ray analysis (SEM-EDAX), photoacoustic Fourier transform infrared spectroscopy (PA-FTIR), thermogravimetric analysis (TGA), modulated differential scanning calorimetry (MDSC), dynamic mechanical analysis (DMA), atomic force microscopy (AFM), transmission electron microscopy (TEM), ^{29}Si solid-state nuclear magnetic resonance (^{29}Si solid-state NMR), small-angle X-ray scattering (SAXS), and wide-angle X-ray diffraction (WAXS).

Experimental Section

Materials. Iotek 4200-Zn−PEAA neutralized by zinc salt and manufactured by EXXON Chemicals was used. The weight percent of acrylic acid in Zn−PEAA is 11%, and 14 mol % of the acrylic acid is neutralized by zinc salt. The metal alkoxide used in our investigation was tetraethyl orthosilicate (TEOS; Aldrich). Butylamine received from Aldrich was used as a catalyst. Solvents used were the mixtures of toluene and n-butanol.

Preparation of the Hybrid. Zn−PEAA was dissolved in the binary solvent mixture to form 10% solution. A TEOS, distilled water, and butylamine mixture was then added into the solution. The content of TEOS in the mixture was 50 wt %. The ratio of TEOS/H_2O is 1:4. The quantity of butylamine was 0.02 g. The reaction lasted for 1 h at 65 °C with stirring. Then, the mixture was poured into the Petri dish. The sample was heated in the oven at 60 °C to accelerate the condensation reaction and aged for 1 week. All the tests were performed 24 h after heat aging.

Sample Characterization. *Spectroscopic Characterization.* PA-FTIR was done using a Nicolet Magna Spectrometer (Model 750) equipped with a MTEC (Model 300) photoacoustic cell. Carbon black was used as reference. Helium was used because of its high thermal conductivity. A gas flow rate of 10 cm^3/s was used. The resolution of 8 cm^{-1}, 256 scans, and mirror velocity of 0.158 cm/s was used for all measurements.

The ^{29}Si solid-state NMR was used to evaluate the structure of silica in the hybrid. Cross-polarization and magic-angle spinning (CP/MAS) were used to obtain the spectra. The spinning rate was 4 kHz. A radio frequency 62.5 kHz was used for cross-polarization and proton decoupling (90° pulse width for ^{1}H = 4 μs). A standard Bruker 4 mm CP/MAS probe was used. The recycle time was 8 s.

Small-angle X-ray scattering (SAXS) data were obtained at room temperature using compression-molded films and a Bruker SAXS instrument. The sample-to-detector distance was 62.7 cm. The X-ray source was from Cu Kα radiation, and the wavelength is 1.54 Å. The scan of 2 Å was from 0.15 to 5°. Wide-angle X-ray diffraction (WAXD) was obtained at room temperature using compression-molded films using a Bruker 5005 X-ray powder diffractometer for the reflected diffraction mode and a Bruker X-ray instrument that consisted of a rotating anode source, pinhole collimation, and a two-dimensional Hi-STAR detector for the transmitted mode experiment.

Microscopic Characterization. SEM-EDAX was used to study the structure and morphology of the hybrid material.

(12) Xie, J.; Zhou, C.; Feng, S.; Wang, X. *J. Appl. Polym. Sci.* **2000**, *75*, 379.
(13) Joly, C.; Smaihi, M.; Porcar, L.; Noble, R. D. *Chem. Mater.* **1999**, *11*, 2331.
(14) Huang, H.-H.; Order, B.; Wilkes, G. L. *Macromolecules* **1987**, *20*, 1322.
(15) Mello, N. C.; Bonagamba, T. J.; Panepucci, H.; Dahmouche, K.; Judeinstein, P.; Aegerter, M. *Macromolecules* **2000**, *33*, 1280.
(16) Materka, L.; Dusek, K.; Plesstil, J.; Kriz, J.; Lednicky, F. *Polymer* **1998**, *40*, 171.
(17) Eisenberg, A.; Kim, J. S. *Introduction to Ionomers*; John Wiley & Sons, Inc.: New York, 1998.
(18) Mauritz, K. A.; Stefanithis, I. D.; Davis, S. V.; Scheetz, R. W.; Pope, R. K.; Wilkes, G. L.; Huang, H.-H. *J. Appl. Polym. Sci.* **1995**, *55*, 181.
(19) Huang, Z.; Qiu, K. *Acta Polym. Sci.* **1997**, *4*, 434.
(20) Siuzdak, D. A.; Mauritz, K. A. *Polym. Prepr., Am. Chem. Soc.* **1997**, *38*, 245.
(21) Zeng, Z.; Wang, S.; Yang, S. *Chem. Mater.* **1999**, *11*, 3365.

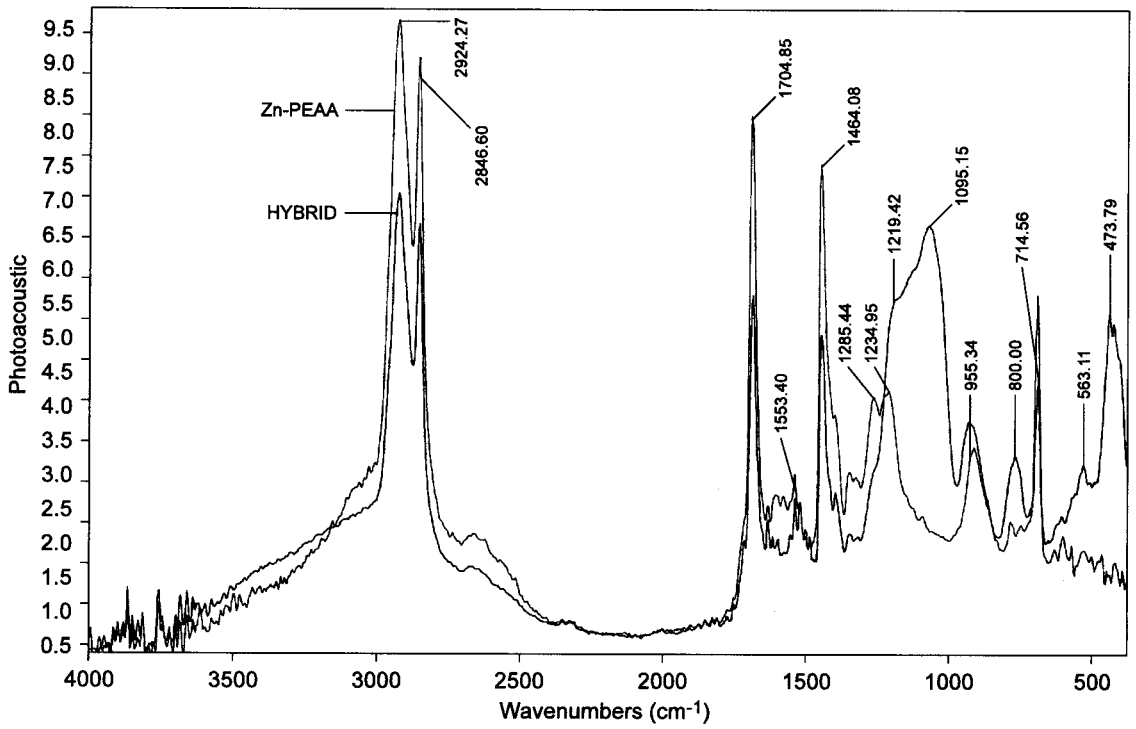

Figure 1. FTIR spectra of ionomer and the hybrid.

The sample was coated with carbon coating before the test. The samples were examined by Hitachi S-800 scanning electron microscope attached with an energy-dispersive X-ray analyzer to determine the elemental composition. Energy-dispersive X-ray was conducted using Cam Scan CS44 scanning electron microscopy operating at an acceleration voltage of 20 kV. All images were scanned using the slow-scan mode for improved clarity. Various magnifications were used to allow for sample images in the range of 300 nm to 300 μm. The EDAX program was used at a resolution of 148.7 V at Mn Kα, with a take off angle of 31.4°, and with a working distance of 37.0 mm, at 10 eV/channel to generate elemental analysis for the residue of the hybrid material.

TEM micrographs were taken on a Philips CM100 transmission electron microscope. X-ray microanalysis (to determine elemental composition) of the samples was performed on a Philips CM200 transmission electron microscope with EDAX DX4 microanalysis equipment.

Atomic force microscopy (AFM) was performed in pulsed force mode (PFM)[22,23] in which mapping of surfaces can be performed using measurement related to local adhesion, elastic, and electrostatic properties. A Witec pulsed force module coupled to a TA Instruments 2990 μ-thermal analyzer was used with a Thermomicroscope Explorer AFM. A tektronix TDS 210 oscilloscope was used to monitor the modulated force vs time and to set up parameters. High-resolution scans were performed on a 5 mm × 5 mm area of the sample. Thermomicroscope's silicon cantilever probe was used, whose resonant frequency is 23−38 kHz and tip radius is 10 nm. The modulation frequency was set at 500 Hz and the amplitude at 5% of maximum. The indentation force signal used was 5 nA.

Thermal Analysis. TGA of the samples was conducted using a TGA 2950 thermal analyzer (TA Instruments) using a conventional (heating rate) mode under either a nitrogen or oxygen atmosphere at a flow rate of 50 mL/min. The mass of samples was used between 10 and 12 mg. The sample was heated from 30 to 900 °C at a heating rate of 10 °C/min, up to 500 °C in nitrogen, and between 500 and 900 °C in oxygen. The onset of degradation, the weight loss due to different ingredients, and the residue remaining at 900 °C were evaluated.

MDSC was performed on a TA 2920 MDSC from TA Instruments Inc. The sample mass was 5−10 mg. Helium with a flow rate of 50 mL/min was purged through the sample. The sample was heated from 30 to 120 °C at a 2 °C/min heating rate, with an amplitude of modulation ± 0.2 °C and a period of 40 s. The samples were also cooled at different cooling rates in DSC mode, and the crystal melting was observed in a subsequent MDSC run.

Mechanical Analysis. Dynamic mechanical properties of the samples were measured using DMA 2980 (TA Instruments). The module DMA multifrequency−multitension mode was used with a static force of 1 N and frequency of 1 Hz. The sample was heated from −150 to +100 °C at a 2 °C/min heating rate. Liquid nitrogen was used to achieve subambient temperature.

Results and Discussion

Effect of the Sol−Gel Reaction on the Structure of the Ionomer. *Spectroscopic Studies.* FTIR spectroscopy was used to analyze the structure and composition of the hybrid. The general reactions that occur during the sol−gel process are shown below

$$n\mathbf{Si(OR)}_4 + 4n\mathrm{H_2O} \rightarrow n\mathrm{Si(OH)_4} + 4n\mathrm{ROH} \quad (1)$$

$$n\mathbf{Si(OH)}_4 \rightarrow n\mathrm{SiO_2} + 2n\mathrm{H_2O} \quad (2)$$

Here the −Si−OH is the key intermediate, being instrumental to the whole process, where the un-ionized carboxyl groups in the ionomer are highly capable of hydrogen bonding and they can form a strong hydrogen bond with the silanol groups (Bronsted acid). The overlaid FTIR spectra of both the ionomer and the hybrid are shown in Figure 1. Table 1 lists the wavenumbers of the ionomer and the hybrid, and their corresponding functional groups. Figure 1 shows two peaks in the range of 2800−3000 cm^{-1} in both cases.

(22) Krotil. H. U.; Stifter, T.; Waschipky, H.; Weishaupt, K.; Hild, S.; Marti, O. *Surf. Interface Anal.* **1999**, *27*, 336.

(23) Miyatani. T.; Horii, M.; Rosa-Zeiser, A.; Fujihira, M.; Marti, O. *Appl. Phys. Lett.* **1997**, *71* (18) 2632.

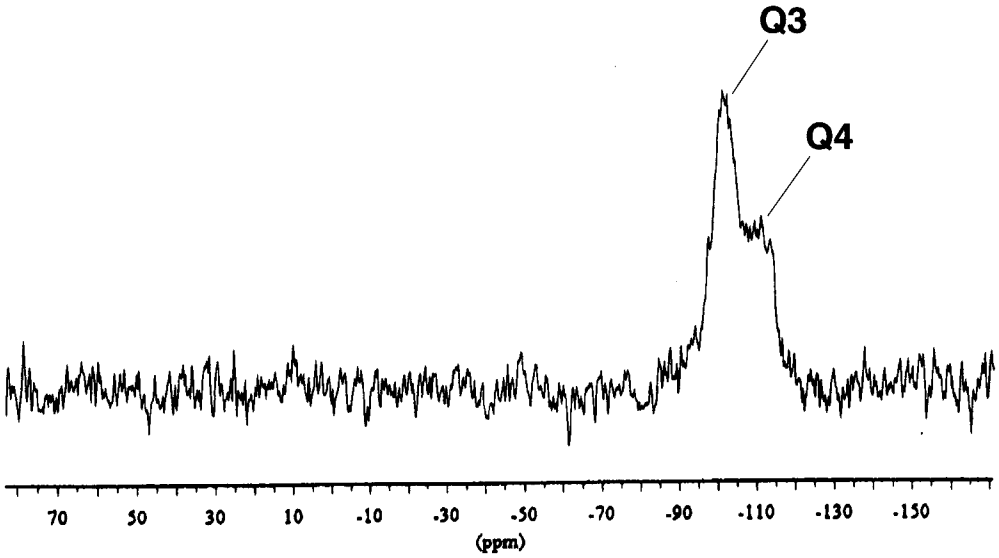

Figure 2. ^{29}Si solid-state NMR spectrum of the hybrid.

Table 1. Peak Assignment from FTIR for the Ionomer and the Hybrid

peak position, cm^{-1}	assignment	
	ionomer	hybrid
2800−3000	$-CH_2-$, $-CH_3$	$-CH_2-$, $-CH_3$
2660	bonded OH in carboxylic acid	bonded OH in carboxylic acid
1700	−COOH	−COOH
1460−1470	$-CH_2-$ bending	$-CH_2-$ bending
1219	ester	
1000−1200		SiOSi asymmetric stretching
955	out-of-plane bend of H bonded OH, COOH	out-of-plane bend of H bonded OH, COOH, SiOH
800		$SiCH_3$ rocking vibration
714	$-(CH_2)_n-$, CH=CH−	$-(CH_2)_n-$, CH=CH−
473		SiOH, SiOSi

This relates to the $-CH_2-$ and $-CH_3$ groups. The positions of these two peaks remain the same for both materials. This indicates that no chemical bond between silicon and these two groups forms after the sol−gel reaction. The band at 1700 cm^{-1} is the C=O stretching mode from the −COOH group. This is noticed in both ionomer and the hybrid samples. This is due to unneutralized acrylic acid in Zn−PEAA. While the transparency of the hybrid is a result of strong organic−inorganic interaction, and a high degree of mixing, no evidence of hydrogen bonding is observed from the FTIR peak position. Several polymers with strong hydrogen acceptor group and capable of forming a hybrid with metal alkoxide are reported in the literature.[24] In those cases a shift in the position of the hydrogen bond forming group is observed. A strong absorption band in the range 1000−1200 cm^{-1} is observed in the hybrid and is ascribed to asymmetric stretching vibrations of the Si−O−Si bonds of the silica component,[25,26] which is produced by in situ complete condensation between SiOR and/or SiOH groups. The shoulder on the left side of this vibration indicates the different substructures between Si−O−Si group, e.g., linear and cyclic (1063 and 1108 cm^{-1}). The absorbance at 945−968 cm^{-1} is ascribed to the −Si−OH vibration, the intensity of which indicates the quantity of the unreacted silanol group. The band at this position is also characteristic of the ethylene−acrylic acid copolymer as is another absorbance band at 800 cm^{-1} which arises from the Si−O bond in the Si−OH group.[27,28] Finally, the peak at 473 cm^{-1} is due to the Si−O−Si bending mode[29] and the Si−OH group. The above results all indicate that not only silica but also other forms of silicon groups are formed via the sol−gel reaction. The existence of the Si−OH group indicates that the condensation reaction was not completely finished.

While FTIR results show that Si−O−Si groups are formed via the sol−gel reaction, the ^{29}Si solid-state NMR result further gives the structure of silica and the degree of silicon condensation. Figure 2 shows the ^{29}Si solid-state NMR result of the hybrid. It shows that two kinds of silicon environments (non- and monohydroxy environments) adjacent to each other in the range of −90 to −115 ppm, which are Q3 and Q4, respectively (a silicon bound to four other silicon through oxygen). The Q3 peak is sharper and taller; the Q4 peak is wider and shorter. The degree of condensation within the SiO_2 particles can be evaluated from the Q4 percent. In the ^{29}Si solid-state NMR spectra, Qn (n = 0, 1, 2, 3, or 4) is used to show un-, mono-, di-, tri-, and tetra-substituted siloxanes [$Si(OSi)_n(OX)_{4-n}$, X = H or C], respectively. The chemical shift (relative to tetramethylsilane) of Qn are about −80, −87, −98, and −108 ppm, respectively, from 1 to 4.[30] In Figure 2, Q3 and Q4 are present, but no Q1 and Q2 are observed. Also, the ^{29}Si solid-state NMR results indicate that the degree of silicon condensation is very high. Similar observations were made for Surlyn−silica hybrid material by Siuzdak et al.[20]

(24) Chujo, Y.; Saegusa, T. *Adv. Polym. Sci.* **1992**, *100*, 11.
(25) Silverstein, R. M.; Bassler, G. C.; Morrill, T. C. *Spectrometric Identification of Organic Compounds*, 5th ed.; John Wiley & Sons, Inc.: New York, 1991; p 91.
(26) Hsiue, G.-H.; Kuo, W.-J.; Huang, Y.-P.; Jeng, R.-J. *Polymer* **2000**, *14*, 2813.
(27) Zhao, Z.; Gao, Z.; Ou, Y.; Qi, Z.; Wang, F. *Acta Polym. Sin.* **1996**, *2*, 228.
(28) Smith, A. L. *Spectrochim. Acta* **1960**, *16*, 87.
(29) Tsao, M.-W.; Pfeifer, K.-H.; Rabolt, J. F. *Macromolecules* **1996**, *29*, 7130.
(30) Joseph, R.; Zhang, S.; Ford, W. T. *Macromolecules* **1996**, *29*, 1305.

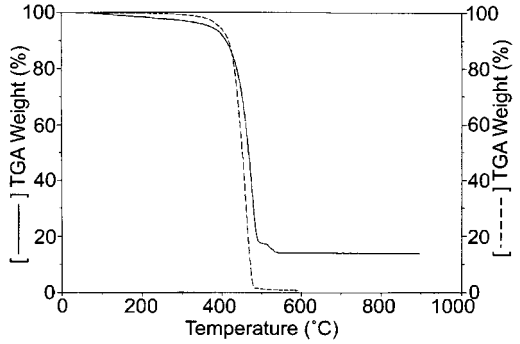

Figure 3. Weight loss vs temperature plot of ionomer and the hybrid.

The effect of the H_2O/TEOS ratio on the sol−gel reaction was examined to investigate the homogeneity of the hybrid. It is found to have a significant effect. A large amount of water is found to cause phase separation during the reaction. When the H_2O/Si ratio is 1, the sample is transparent. When the ratio is increased to 5, the sample loses transparency. When the ratio is equal to or greater than 10, silica particles appear. The higher the ratio, the more silica particles can be seen. Increasing the amount of water speeds up the hydrolysis reaction. During aging in the oven, more silica formed and aggregated, indicating the fact that the particle size of silica increased with increasing H_2O/Si ratio.

To confirm the nature of the interaction in the hybrid, an equilibrium swelling experiment was performed in the same solvent used for making ionomer solution. Disks were made from the hybrid and kept in the solvent at room temperature and at 65 °C for 7 days. It is interesting to note that the whole sample was swollen, indicating that there is a degree of cross-linking between the organic and inorganic phases. Currently, more work is underway to establish the cross-link density. The existence of the Q3 peak and a strong interface as discussed in the DMA section confirms the presence of a −Si−O−C bond in the hybrid associated with iono-covalent interaction.

Compositional Analysis and Thermal Stability of the Hybrid. TGA was used to obtain the percent composition of silica in the hybrid and the thermal stability of the samples. Figure 3 overlays the weight loss curves of the hybrid material and the Zn−PEAA. The solid line shows the hybrid curve; the dashed line, the Zn−PEAA curve. It is obvious that the decomposition temperature of the hybrid shifts toward the higher temperature. The decomposition temperature is 458 °C for Zn−PEAA and 468 °C for the hybrid. This indicates that the thermal stability of Zn−PEAA increases after the sol−gel reaction. Wen and Wilkes[1] reported that the existence of inorganic materials in polymer materials could enhance the thermal stability of the composite. In the present case also, the thermal stability increases due to the presence of the inorganic phase and its interaction with the ionomer. Figure 4 shows the weight loss vs temperature and the derivative weight loss vs temperature of the hybrid material. The derivative weight loss curve shows two peaks. The main peak crosses the temperature range from 300 to 510 °C, which relates to the decomposition of the polymer. Below 300 °C, there is a small weight change, corresponding to the low molecular weight byproducts, the solvents, and

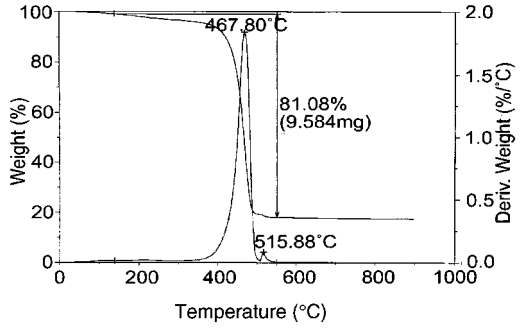

Figure 4. TG and DTG curves of the hybrid.

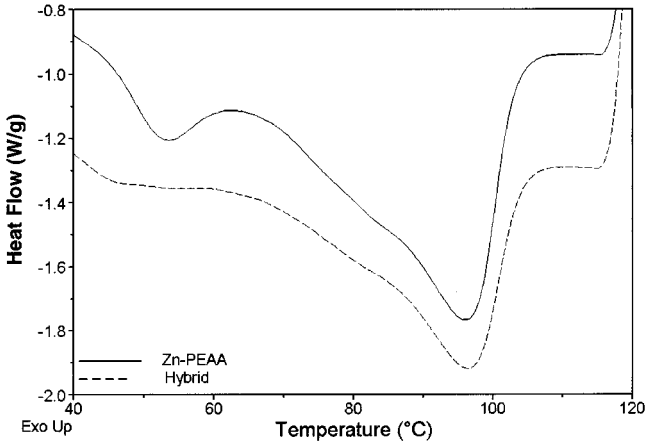

Figure 5. DSC thermograms of ionomer and the hybrid.

further condensation of silica.[31] On the right-hand side of the main peak, there is a small peak. This is attributed to either removal of a residual ethoxy group or dehydroxylation of the silica surface after the decomposition of polymer. However, it must be pointed out that the purge gas was changed at 500 °C, and no such peak is observed in pure ionomer. The weight-loss temperature curve shows that the residue left after 900 °C is about 19%. The residue was further analyzed by SEM/ EDAX to characterize the morphology and elemental analysis. It is found to be silica.

The theoretical silica content of the sample is also calculated from the ratio of $SiO_2/Si(OEt)_4$ and compared with the experimental value obtained from TGA. If a complete hydrolysis of $Si(OEt)_4$ occurs, the silica content of the sample would be 28 wt %. However, in the present case, the oxide content is 19 wt %, indicating a yield of 66%. The variation in the oxide content in the hybrid is either due to the incomplete hydrolysis of the ethoxy group or condensation of the silanol group. While the latter is observed from our FTIR and ^{29}Si NMR results, the incomplete hydrolysis is also thought to be a contributing factor to the total oxide variation.

Morphological Study. DSC and MDSC were used to monitor the transition behavior of the samples and to obtain the crystallinity. Figure 5 shows the DSC results of the ionomer and the hybrid material from the first heating run at 20 °C/min heating rate. In each curve, two endothermic peaks are observed. The high-temperature peak at about 95 °C represents the melting of polyethylene; the low-temperature peak at about 48 °C is due to the melting of the clusters in ionomer.[32] It

(31) Wang, S.; Ahmad, Z.; Mark, J. E. *Chem. Mater.* **1994**, *6*, 943.

Table 2. MDSC Results of Zn−PEAA and the Hybrid

	cooling rate, °C/min	revers heat, J/g	nonrevers heat, J/g	heat flow, J/g	% crystallinity	melting temp, °C
Zn−PEAA	0.5	12.1	52.6	64.7	22.3	95.4
	2	15.3	45.4	60.7	20.9	94.5
	5	20.5	40.4	60.8	20.9	94.7
hybrid	0.5	16.8	34.6	51.4	17.7	95.2
	2	18.4	26.2	44.6	15.4	94.4
	5	22.6	25.7	48.3	16.6	94.1

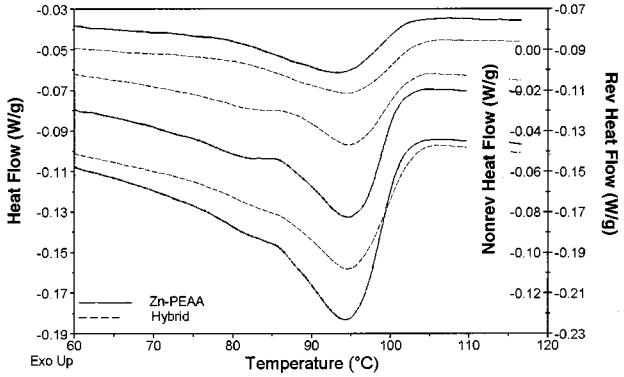

Figure 6. MDSC thermograms of ionomer and the hybrid.

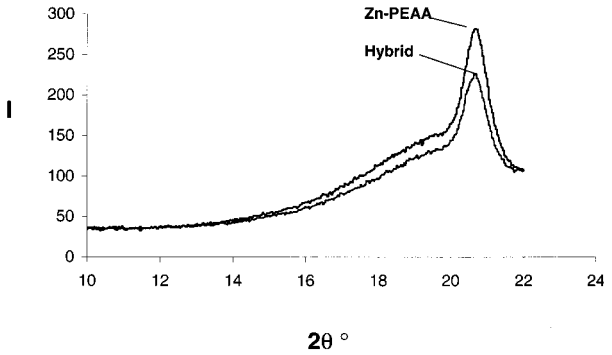

Figure 7. Intensity I vs 2θ plot from WAXS of ionomer and the hybrid.

is obvious that the cluster melting peak is sharper and bigger in the ionomer than in the hybrid material. This represents a less ordered structure of the clusters after the sol−gel reaction and insertion of silica particles in the cluster via the reaction. The total heat flow of the hybrid material is reduced compared to that of Zn−PEAA after the sol−gel process.

Figure 6 shows the MDSC thermograms of the hybrid and the ionomer at a 2 °C/min heating rate, the total heat flow (the bottom curves), and the reversing (top) and nonreversing heat flow curves (middle) of Zn−PEAA and the hybrid. The three heat flow curves show primarily the melting of the polyethylene part of the samples. Thus, it is clear that the melting of polyethylene occurs in the reversing and nonreversing signals. A shoulder appears on the left-hand side of the main melting peak in the total heat flow and nonreversing heat flow. This is due to the melting of folded chains. By comparing these two samples, it is obvious that the shoulder size is bigger in Zn-PEAA than in the hybrid. Kovacs and Gonthier[33] and recently Cheng and Chen[34] explained the shoulder in a melting process not only does correspond to different types of folding but also can be due to different morphologies present in the system. Table 2 lists the MDSC results at different cooling rates for Zn−PEAA and the hybrid. It is clear from the table that the total melting behavior of Zn−PEAA does not change under different cooling rates after the sol−gel reaction. When the total heat flow is resolved, two components appear indicating that melting of the hybrid also occurs in the reversing as well as nonreversing heat flow. The fraction of melting in both these signals depends on various experimental parameters such as modulation amplitude, period, underlying heating rate, and sample thickness, etc. Under different cooling rates, the contributions of the reversing heat flow and the nonreversing heat flow change but the total heat flow varies marginally. Such results show that the introduction of silica increases the reversing heat flow, but decreases the nonreversing part and the total crystallinity. In general, the kinetic component of the heat flow increases with increasing regularity of a system. This could be related to the entanglement density of the melt. In linear polymer melt entanglement density increases because of its favorable structure. However, in a branched polymer, that does not occur as branching acts as anchoring points preventing coiling and melting is almost 100% reversible. It is possible that both ionization and the sol−gel reaction reduce or restrict the ease of spherulite formation of the PE part of the ionomer. The total crystallinity of this part can be calculated from the ratio of the observed heat flow value to the total heat flow of the 100% PE value (the literature value for 100% crystalline PE is 290 J/g). The table shows that the crystallinity of the hybrid is about 17.7% at a 0.5 °C/min cooling rate, while the crystallinity of Zn−PEAA is 22.3% at the same cooling rate.

WAXS can be used to monitor the crystallinity and polymer morphology. In our recent publication,[32] the details of ionomer's crystallinity using MDSC and WAXS have been discussed. Figure 7 shows the WAXS profile of Zn−PEAA. It shows that there is a sharp peak at about 20.7°, which relates to the crystal part of polyethylene. At the left side of the sharp peak, there is a shoulder corresponding to the amorphous phase of polyethylene. Using the peak areas, the crystallinity was calculated. And the crystallinity of Zn−PEAA is 24% by WAXS,[32] which is in good agreement with the MDSC result. The WAXS of the hybrid had lower intensity and a broad peak in the same region at 2θ of 20.7° (d spacing, 4.36 Å). Additionally, Figure 7 shows the crystal peak does not shift via the sol−gel reaction, but the intensity decreases. This indicates that the crystallinity of the hybrid is lower than that of Zn−PEAA but the d spacing does not change. This result agrees with the MDSC result that the introduction of

(32) Gao, Y.; Choudhury, N. R.; Dutta, N.; Matisons, J. Submitted for publication in *Thermochim. Acta*. Also presented at: 24th Australian Polymer Symposium; Beechworth, Victoria, Australia, Feb 4−8, 2001.

(33) Kovacs, A. J.; Gonthier, A.; Straupe, C. *J. Polym. Sci., Polym. Symp.* **1975**, *50*, 283.

(34) Cheng, S. Z. D.; Chen, J. *J. Polym. Sci., Part B: Polym. Phys.* **1991**, *29*, 311.

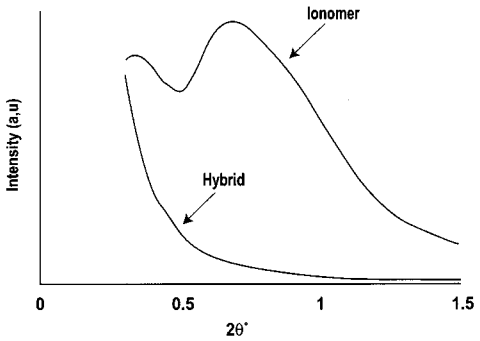

Figure 8. SAXS scattering profile of ionomer and the hybrid.

silica decreases the ionomer's total crystallinity but the melting point does not change. The diffractogram also shows a specific but a broad peak below 5˚ (~4˚). This is due to the clusters being areas of higher electron density than their surrounding. In X-ray diffraction, the plot of intensity vs 2θ will show ionic microstructure from peaks in the low-angle region and a crystal pattern from the higher θ region. The SAXS profiles of the ionomer and the hybrid are shown in Figure 8. The significant difference in the scattering profile is evident from the figure. In the pure ionomer, an upturn followed by a sharp peak due to ionic cluster is clearly seen. The existence of ionic peak (at $2\theta = 0.69^\circ$ and d spacing = 127 Å) reveals the inhomogeneity in electron density in the ionomer. It is interesting to note that this SAXS maximum is absent in the sol−gel hybrid material. This could be due to the fact that water completely disrupts the ionic peak during the sol−gel reaction. However, it must be mentioned here that no water was detected in this sample after reaction from thermogravimetric analysis or infrared spectroscopy. The disappearance of this long period after the sol−gel reaction thus indicates the fact that penetration of silica occurs uniformly in a very small scale due to strong ionic interaction of the ionomer and the silanol group of silica. The d value of the hybrid is found to be 294 Å compared to ionomer's d value of 267.4 Å. It is ascribed to a considerably large size of cluster morphology due to the incorporation of silica; in that case, the scattering maximum might be very close to beam stop affecting resolution. It is noteworthy that the near zero angle, long-range order or the upturn in the hybrid could be due to factors such as the existence of multiplets or isolated ionic groups rather than an intercrystallite scattering profile.

Microscopic Observations of Morphological Features. Scanning electron microscopy was used to study the morphology of the hybrid residue obtained from the TGA. Figure 9 and Figure 10 show the SEM (SEM at different magnifications) images of the TGA residue of the hybrid material. The silica network morphology is clearly observed in the hybrid. Figure 9 shows that a uniform network of silica was formed in the hybrid. The silicon compound formed via the sol−gel process is dispersed in Zn−PEAA on a nanoscopic level. Figure 10 is the micrograph of the same material at high magnification. This figure demonstrates the morphology of the silica network clearly via the sol−gel process. Silica particles are spherical in shape with a regular distribution. The average particle size is about 50−60 nm. Figure 11 displays the EDAX elemental mapping of the hybrid residue obtained from TGA. The result

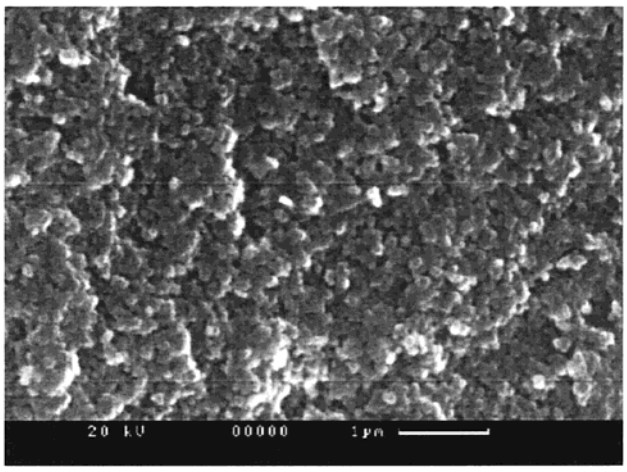

Figure 9. Morphology of the silica network from the TGA residue of the hybrid obtained at 900 ˚C.

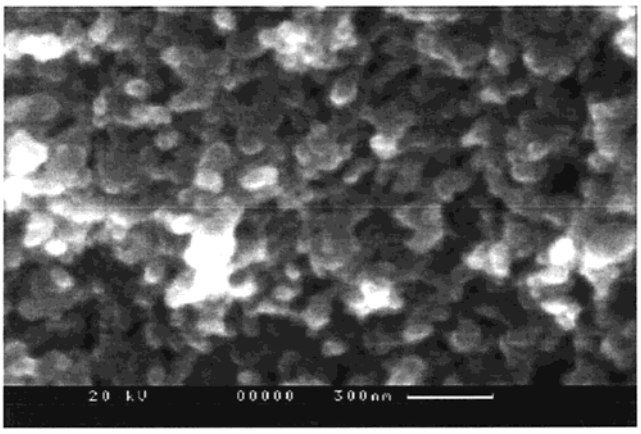

Figure 10. Scanning electron micrograph of the TGA residue of the hybrid at high magnification.

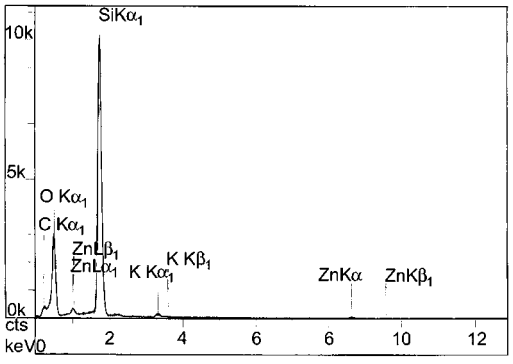

Figure 11. EDAX of the TGA residue.

shows that the stoichiometric ratio of silicon and oxygen to be Si/O > 3. This indicates that not only silica but also other silicon compounds were present after the sol−gel process. This is in line with the FTIR and ^{29}Si solid-state NMR observations. The presence of carbon is from the carbon coating used for SEM sample preparation.

TEM was also used to obtain the morphology and microstructure of the hybrid. Figure 12 shows the photomicrograph of the hybrid. The dark area on the figure shows a spherical silica nanoparticle. It is obvious that very fine silica particles are dispersed homogeneously in the polymer matrix after the sol−gel reaction. The TEM result confirms the SEM-EDAX results.

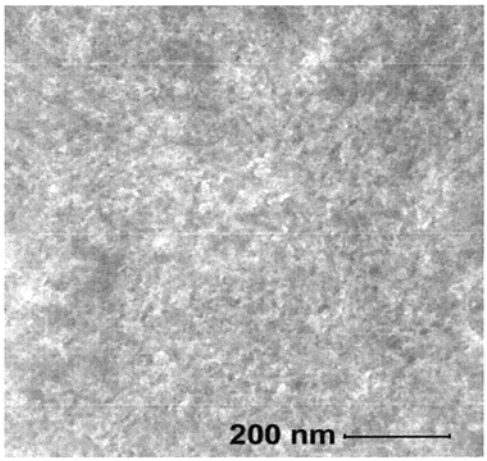

Figure 12. Morphology of the hybrid from TEM.

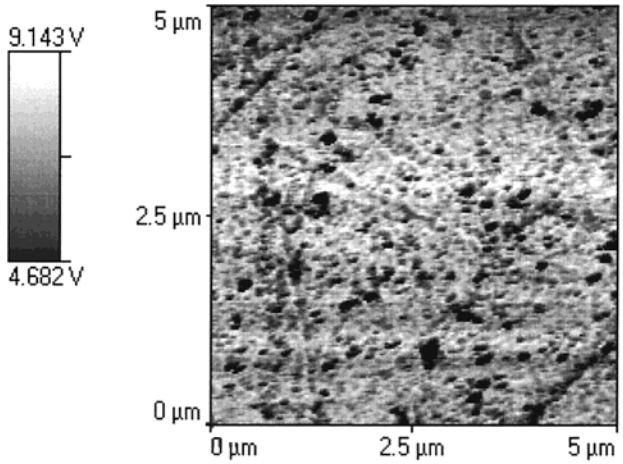

Figure 13. Pulsed force micrographic image of the hybrid.

Figure 13 shows the pull-off force image for the hybrid at room temperature. It shows uniform distribution of low-adhesion and high-stiffness areas, which are dark particles in a high-adhesion soft continuous matrix (low stiffness). The average particle diameter ranges from 50 to 60 nm. Thus the morphological information obtained from SEM of the TGA residue and the TEM of the hybrid are in line with pulsed force mode micrographic information.

Mechanical Properties of the Hybrid. DMA is a very useful tool for obtaining the dynamic mechanical properties of polymers. Figure 14 shows the plot of the storage modulus (the top curves) and the damping curves (bottom) of the ionomer and the hybrid. The modulus and the damping curves show three distinct transitions in the entire range: a broad transition with a peak maximum of 29 °C for pure ionomer and 34 °C for the hybrid. This peak is attributed to the cluster's transition. The nature of the peak is similar in both cases; in other words it does not show broadening. In a study, MacKnight et al.[35] pointed out that there are four transitions of the ethylene ionomers: the α transition (>50 ˚C) related to motions in the ionic phase, the β' transition (∼50 ˚C) to the micro-Brownian motions of chain segments (glass transition), the β transition (∼0 ˚C) due to the relaxation of polyethylene branches,

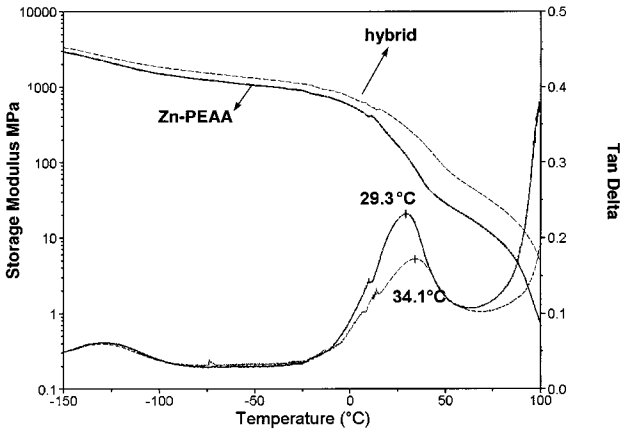

Figure 14. Plot of storage moduli and tan δ vs temperature of the ionomer and the hybrid.

and the γ transition (∼−130 ˚C) to polyethylene crankshaft rotation transition. In the present case, a shoulder to the broad transition is observed at ∼−5˚ for both samples which is the β transition typical of branched low-density polyethylene, while the γ transition at −128 ˚C shows no change with the sol−gel reaction. The broad cluster transition and the shoulder shift to higher temperature, indicating restricted melting in this region. The storage modulus of the hybrid is also higher than that of pure ionomer with the growth of the silica phase. Figure 14 shows that the storage modulus decreases with increasing temperature. It is interesting to note that a rubbery plateau occurs after clusters transition and the storage modulus value of the hybrid is significantly higher (1 order magnitude) than that of pure ionomer, due to the presence of silica. It must be pointed out here that the storage modulus values of the two samples show a large difference from 50 ˚C onward. The difference in the modulus values between −25 ˚C and +50 ˚C can be regarded as a measure of gel content. Also it indicates a strong polymer−silica interface with strong specific interaction. Since the γ transitions in this case do not show any broadening as observed in the carbon black filled system due to wide distribution of interaction energy, it is believed that there exists a fixed bond energy for silica−ionomer interaction with a narrow distribution. This also indicates that the γ transition is independent of the silica existence. At 100 ˚C, the storage modulus is close to zero. This is caused by melting of the samples. Thus, it is clear that the introduction of silica particles on a nanoscopic level affects primarily the molecular motion of the chain segments present in the cluster.

Conclusions

Zn−PEAA−silica hybrid material was synthesized using the sol−gel reaction. FTIR and ^{29}Si solid-state NMR results prove that silica is formed via the sol−gel reaction. TGA results show that the proportion of silica is 19%. The sample is transparent. This indicates that no phase separation exists between ionomer and silica. TEM, SEM-EDAX, and PFM results prove that the silica particle size is in the nanoscopic level and is smaller than the wavelength of visible light. The

(35) MacKnight, W. J.; Mckenma, L. W.; Read, B. E. *J. Appl. Phys.* **1967**, *38*, 4208.

microscopy results also show that nanosized silica disperses homogeneously in the polymer matrix. Thermal analysis shows that the introduction of the nanosize silica improves the thermal stability of Zn−PEAA. The crystallinity of the hybrid is lower than Zn−PEAA as seen from MDSC and WAXS. The SAXS result proves that silica influences the microphase separated domains via the sol−gel reaction. From dynamic mechanical analysis, it is clear that the molecular motion of the chain segment in the cluster is influenced by the growth of silica particles.

Acknowledgment. The authors are thankful to Mr. Clint Gamlin for performing the WAXS and SAXS experiments and also to Prof. Bob Weiss of the University of Connecticut for giving access to the equipment.

CM010179S